

Helicopter Rotor Unsteady Aerodynamics

Charles O'Neill

April 26, 2002

Helicopters can't fly; they're just so ugly the earth repels them.

1 Introduction

Unsteady helicopter rotor aerodynamics are complicated. This paper reviews some of the fundamentals and newer developments of unsteady helicopter aerodynamics.

Rotor flow is beautiful and complex. Visualizing rotor flow allows for an appreciation of the following theories and solution attempts as well as nature's complexities. The flow through a helicopter rotor with forward motion is shown in Figure 1. The rotor is rotating horizontally along the right hand side. Notice the regular rake inlet and the regular rotational outlet! The next photo, Figure 2, shows a full size helicopter flying through five smoke streams. Once again, the regular inlet is transformed to a rotating flow field.

This paper will discuss four areas of unsteady helicopter rotor aerodynamics. First, this paper discusses the classical harmonic solutions to rotational aerodynamics and their relationship to the fundamental Theodorsen solution. Second, modern solution techniques are discussed. Finally, the paper describes wake interactions and their noise production implications.

2 Harmonic Rotor Aerodynamics

The early representations of unsteady rotor aerodynamics reduced the rotor's flow field to two dimensions. The Theodorsen and Sears functions form the underlying foundation for these rotational approximations. The Isaacs and Loewy functions are the classical two dimensional unsteady rotor functions.

2.1 Theodorsen and Sears

The classic 2D unsteady approximations are the Theodorsen and Sears functions. The Theodorsen function describes an airfoil oscillating in pitch and plunge. The Sears function describes an airfoil with a transverse harmonic 'gust'. These functions were derived from a non-rotating reference frame. However, they provide a convenient reference for rotating flows. While changing to rotational coordinates creates some confusion as to how boundary

condition motions are referenced and measured, Johnson[1] shows the proper derivation of the boundary conditions. The Theodorsen and Sears functions are given below.

$$C(k) = \frac{H_1^{(2)}(k)}{H_1^{(2)}(k) + iH_0^{(2)}(k)} \quad S(k) = \frac{1}{\pi \frac{k}{2} (H_0^{(2)}(k) - iH_1^{(2)}(k))}$$

2.2 Isaacs (1946)

The Isaacs problem[2] describes an airfoil with an axially harmonic free-stream velocity. The physical geometry is shown in Figure 3.

The Isaacs problem corresponds to a rotating rotor blade moving into a free stream velocity. The Isaacs problem is derived in a 2D coordinate system like the Theodorsen and Sears problems. When second order terms are dropped, the Isaacs problem reduces to a function of the airfoil's geometry and the Theodorsen function. This is expected since the Isaacs derivation is based on a modified Theodorsen derivation.

2.3 Loewy Function (1957)

The Loewy function[3] describes a 2D rotor with harmonically occurring blade passages. Shed vorticity is placed on discrete vertical steps. The resulting physical flow domain, Figure 4, describes a rotor with a constant axial inlet velocity.

The derivation for the Loewy function is complicated by the inflow velocity. Figure 4 also gives a description of the rotor's shed wake. Clearly even though the inflow is constant, the overall shed wake geometry depends on the inflow rate. A higher inflow spreads out the wake more than a low inflow. Thus we expect the Loewy function to asymptotically approach the Theodorsen function for very large inflow rates.

The Loewy function derivation is similar to the Theodorsen function except that the shed wake wraps along an infinite line and discretely shifts downwards instead of convecting downstream. This downwards shift accounts for the rotor inflow.

The Loewy function in terms of Hankel functions is,

$$C = \frac{H_1^{(2)} + 2J_1^{(2)}W}{H_1^{(2)} + iH_0^{(2)} + 2(J_1 + iJ_0)W}$$

where a vorticity weighting factor, W, is defined for a quasi-single blade as

$$W = \frac{1}{e^{kh/b} \cdot e^{i2\pi\omega/\Omega} - 1}$$

Comparing the Loewy function to the Theodorsen function shows that all of the additions are scaled by the weighting factor W. For a large wake spacing, $W \rightarrow 0$, the Loewy function reduces to the Theodorsen function as we predicted. The Loewy function is restricted to a positive downwards influx velocity, h/b , both mathematically and physically due to blade wake interactions.

The Loewy lift deficiency function is plotted against reduced frequency for various h/b ratios in Figure 5(a). The thicker line indicates the Theodorsen function and the Loewy

function for large h/b . For low inflow rates and thus low h/b ratios, the lift deficiency strongly depends on reduced frequency. Reduced frequencies around 0, 4, 7, ... have a lift deficiency of almost zero!

Figure 5(b) plots the Loewy function for reduced frequency for various rotor phasing angles ω/Ω . For low reduced frequencies, the ratio of rotor rotation rate, Ω , to rotor frequency, k , drastically changes the Loewy function. The oscillations eventually approach the Theodorsen value of 0.5 for large reduced frequencies.

Overall, the Loewy function attempts a 2D representation of a rotating rotor's unsteady flow field. The lift deficiency function resembles the Theodorsen function. For high inflow rates, the Loewy function approaching the Theodorsen results. The most important result from Loewy is that the wake geometry and phasing is the primary cause of unsteady rotor loading. Any effective theory must describe the wake geometry.

2.4 Cascade Theory

Assuming a cascade of rotor blades provides an improvement over the Loewy assumption of infinite rows of shed vorticity. Dinyavari and Friedmann [4] created a modified Loewy theory based on cascades of shed vorticity with finite length. Figure 6 shows the cascade geometry. Notice that this method is still based on frequency analysis. A frequency plot of the real part of lift deficiency is shown in Figure 6. Notice that this theory reduces to the Theodorsen result for 0 wake layers. This theory also matches the Loewy theory for low reduced frequencies ($k < 1$). This low frequency match suggests that the upstream infinite vortex lines in Loewy's theory only corresponds to reality in the long wavelength limit.

2.5 Miller (1962)

Miller's theory describes a three dimensional rotating rotor. The theory represents the wake as a cylindrical shell of shed vorticity. Figure 7 shows the geometry domain.

From Miller[5], the lift deficiency function is

$$\frac{L}{L_{qs}} = \frac{1}{1 + \frac{\sigma\pi}{4\lambda}}$$

where σ is the blade solidity and λ is the mean blade inflow. Figure 7 shows the lift deficiency function for various solidity ratios. The Miller theory does not contain rotor frequency information! Johnson [6] discusses some of the implications of Miller's results. In particular, the inflow velocity is no longer steady.

While the Miller theory represents a three dimensional rotor wake, it can not predict unsteady rotor performance with forward motion. The Miller theory accounts for influx and three dimensional cylindrical wakes but not in-plane (forward) motion.

2.6 Induced Flow Models

Numerous people suggested improvements to the Miller method based on harmonic theory. Peters[7] presents a model based on coupled inflow and harmonic blade theories. The rotor and wake aerodynamics are split into coupled finite state equations. Peters expounds the

advantages as a flexible and adaptable theory that “recovers other theories” and matches experimental data. This theory also allows limited forward motion. Models similar to the Peters theory have extended the physical assumptions of a harmonic approach to the limit. Better rotor predictions will require better physical modeling of the wake.

3 Modern Solution Methods

The helicopter rotor operates in a three dimensional space. The previous methods were based on a harmonic approach. More sophisticated methods are based on tracking and coupling the rotor and wake aerodynamics.

3.1 Discrete Vortex Methods

The discrete vortex approach to unsteady aerodynamics involves discretizing and tracing the shed vorticity. These methods are based on Prandtl’s lifting line theory or a similar bound-shed vortex method. The fundamental wake geometry is a shed sheet of vorticity coming off the entire rotor blade. Figure 8(a) shows an idealized view of the shed wake. These methods are capable of forward flight analysis.

3.1.1 Piziali and Landgrebe

Piziali’s method consists of a rotor shedding discrete sheets of vorticity. Figure 8(b) shows the discrete sheet geometry. Notice that the sheets are assumed rigid which assumes that the shed vortices do not affect each other. Not surprisingly, the Piziali method does not accurately predict the rotor aerodynamics[8]. The flow field around a rotor contains too much concentrated vorticity to allow for a rigid wake.

Landgrebe’s method extends the Piziali method by (correctly) assuming that the shed vortices affect and distort each other. This addition to the problem physics allowed a much better correlation to experiments. Additionally, Landgrebe’s method predicts that the rotor’s wake changes for forward flight. The wake coming off the front part of the rotor disk is sucked upwards; whereas the rear wake is pushed downwards. Bramwell[8] surmised that roughness in certain flight conditions might be caused by the forward wake being sucked into the rotor blades. The Landgrebe method also predicts that wakes from forward moving rotors eventually roll up into two tip vortices. Thus the far field of a forward moving rotor resembles the bound and tip vortices of a fixed wing aircraft. Figure 9(a) shows the downstream wake in a hover for the Landgrebe method (left) and a rigid wake approximation (right). The Landgrebe approximation appears to change the shed vortex frequency as a function of span wise location due to a rotationally induced differential velocity.

3.1.2 Miller and Bliss Periodic Method

Miller and Bliss[9] presented an accelerated technique for solving rotational discrete vortex systems with a periodic-solution method. The fundamental flow solver remains similar to the Landgrebe method; however, the solver assumes a periodic steady state wake structure. Obviously, the main disadvantage is that the solution technique ignoring the any transient

wake components. The authors claim that their method allows for better solutions at low inflow rates due to poor convergence behavior of time marching approaches[9]. Figure 9(b) shows the periodic wake for a forward flight condition. Notice that the wake structure is consistent with the tip roll-up and the wake movement conclusions of Landgrebe.

3.2 Computational Fluid Dynamics

The modern trend in unsteady aerodynamic predictions is computational fluid dynamics. In general, CFD codes solve either the inviscid Euler equations or the viscous Navier-Stokes equations. This method allows for superior predictions by allowing grid refinement in high gradient areas to capture shocks and vortices. CFD results allow for arbitrary geometries and flow conditions; however, one drawback to CFD is the massive computational power and time required. A more subtle problem exists with dissipation and grid refinement; both decrease the solution accuracy. The implementation of CFD from the governing equations takes many forms and is beyond this paper's scope. Figure 10 shows a CFD solution for a forward moving rotor. For this testcase, Conlisk reported that: "The complete unsteady calculation takes a total of 45 hours on a single-processor CPU time on Cray C-90 supercomputer and generates 40 Gb of flowfield data". Clearly, CFD is a brute force approach.

4 Wake Interactions

Wake interactions are an inescapable truth of rotating aerodynamics. Rotors create and ingest vortical structures. Currently, blade vortex interaction (BVI) is a busy research area for unsteady aerodynamics. Scores of papers address this topic. As we saw from the Loewy theory, knowing the wake geometry is critical. For all except the special case of hovering, blade vortex interactions occur. Figure 11(a) shows a typical blade-vortex interaction pattern for a descending rotor. An idealized wake pattern for a rotor in forward motion is given in Figure 11(b). To solve a general helicopter unsteady problem, an effective general prediction method must account for wake interactions .

4.1 Theoretical Wake Interaction

Theoretical studies of wake interactions started with the Sears function for a harmonically variable gust passage. Changing the gust properties allows for a simple estimation of rotor blade response. The early wake studies focused on gusts. Later methods studied blade-vortex interactions.

4.1.1 Semi-Infinite Wing Gust Passage

Chu and Widnall[10] present an oblique gust passage theory for semi-infinite wings based on lifting surfaces. Figure 11(c) shows the problem geometry. As expected, they found that gusts modify the wing tip loading distribution. Because a lifting surface theory is used, an arbitrary wing shape is allowed. Figure 11(d) shows the wingtip lift distribution for 4 gust wavenumbers. For higher wavenumbers, k , the wingtip shape (parabola vs square) becomes less important. Thus Chu and Widnall conclude that the lift distribution in a gust is mainly

influenced by the low wavenumber gust components[10]. This is consistent with the Sears problem where high frequencies tend towards zero lift. This gust passage problem is revisited by Martinez and Widnall[11] for oblique gusts in subsonic flows.

4.1.2 Vortex Cutting

The interactions of rotor blades and vortices make vortex cutting important. Vortex cutting occurs regularly in helicopters due to the proximity of blades to the shed wake. Marshall[12] provides a solution to a horizontal blade intersecting a vertical vortex. The study finds that the blade-vortex interaction produces an vortex expansion wave emanating from the airfoil. Marshall also predicts a vortex expansion on the airfoil pressure side and a contraction on the suction side. This theory also predicts a disturbance proportional to freestream velocity over the vortex core diameter. Tighter vortices produce more intense blade-vortex interactions. Interestingly, Marshall notes that his vortex cutting governing equations resemble those for a shock tube[12].

4.2 Computational Wake Interaction

Most recent wake interaction research is done computationally. Computational work has the advantage of arbitrary geometries and automatic visualization; however, the fundamental physics are often not as clear. Traditional wake interactions are usually sufficiently predicted by theory. Blade-vortex interactions (BVI), which are much more complicated, are left to computational methods.

A combined experimental, computational BVI study is presented in Lee and Bershader[13]. Their study determines the structure of a typical shed vortex. This vortex is made to impact a 2D airfoil. Figure 12 shows a visual time history and experimental-computational correlation for the blade-vortex interaction. The blade leading edge geometry exerts the strongest influence on the interaction. Notice the interaction generated sound wave. Lee and Bershader state that the computational simulation always under predicted BVI surface pressures[13].

A BVI for a 3D airfoil is presented in Marshall and Grant[14]. For this study, a vortex ring impacts the airfoil as shown in Figure 13. Notice that the vortex rotational part causes two V shaped leading edge pressure distributions of positive and negative pressures.

4.3 Rotor Noise

Rotor noise is invariably tied to wake and blade-vortex interactions. The field of helicopter noise and especially rotary noise contains hundreds of reports. Farassat[15] provides a review of current (1980) helicopter acoustic prediction methods. Unsteady events, particularly blade-vortex interactions, cause intense helicopter noises.

4.3.1 Tip Mach Number

Schmitz[16] states that numerous experiments show that “BVI noise radiation is known to exhibit a strong dependence on Mach number”. This is expected since the wave propagation off the rotor coalesce to form a shock wave as Mach number increases. Figure 14 shows a schematic view of wave propagation from the advancing rotor blade.

4.3.2 Blade Vortex Interactions

Blade-vortex interactions cause the most intense noises and is caused by the acoustic response to unsteady lift. The literature often refers to BVI as blade-slap. Blade-slap usually occurs in forward flight conditions when the wake is re-ingested. Thus, descending flight and the landing rotation are the most likely conditions for BVI and blade-slap. Schmitz[16] finds that a dipole model adequately describes the directivity of BVI noise. In Schmitz's study, the blade-vortex interactions occurred with 4 wakes (marked 1-4 in Figure 15). Figure 15 gives the directional noise level for each of the 4 wakes. Clearly, the most intense noise occurs off the rotor's leading edge and tip as it intersects the wake.

Wake interactions are still being investigated. Glegg in 1999[17] predicted that blade-wake interaction noise is caused by the rotor blades passing through the turbulent tip vortices. Since turbulence is already a complicated subject, unsteady blade wake interactions will be studied will into the future.

5 Conclusions

Unsteady helicopter aerodynamics are complicated. An understanding of the governing physics is possible by isolating simplified systems. Early contributions were based on harmonic analysis. These methods predicted the basic governing fluid physics and warned about blade-wake interactions. Most modern solutions are based on discrete flow representations and computational solutions. These solutions allowed high resolution studies of fluid flow at the expense of physical insight. These discrete flow methods confirmed the blade-wake interaction sensitivities. Blade-wake interactions are shown to create intense and directional disturbances.

The helicopter rotor is an fundamentally unsteady aerodynamic process. Rotor analysis goes from simple 1D shed vorticity models to fully 3D transient turbulent experiments. While the fundamentals of unsteady rotor flow are known, an overall theory with a closed form solution is clearly impossible. Further developments in unsteady helicopter aerodynamics will continue as long as the helicopter is a viable transportation vehicle.

References

- [1] W. Johnson, “Application of unsteady airfoil theory to rotary wings,” *Journal of Aircraft*, vol. 17, pp. 285–286, April 1980.
- [2] R. Isaacs, “Airfoil theory for rotary wing aircraft,” *Journal of the Aeronautical Sciences*, vol. 13, pp. 218–220, April 1946.
- [3] R. G. Loewy, “A two-dimensional approximation to the unsteady aerodynamics of rotary wings,” *Journal of the Aeronautical Sciences*, vol. 24, pp. 81–92,144, February 1957.
- [4] M. A. H. Dinyavari and P. Friedmann, “Time domain unsteady incompressible cascade airfoil theory for helicopter rotors in hover,” *AIAA Journal*, vol. 27, pp. 257–267, March 89.
- [5] R. H. Miller, “Unsteady air loads on helicopter rotor blades,” *Journal of The Royal Aeronautical Society*, vol. 68, pp. 217–228, April 1964.
- [6] W. Johnson, *Helicopter Theory*. Princeton, New Jersey: Princeton University Press, 1980.
- [7] D. A. Peters, D. D. Boyd, and C. J. He, “Finite-state induced-flow model for rotors in hover and forward flight,” *Journal of the American Helicopter Society*, vol. 34, pp. 5–16, October 1989.
- [8] A. R. S. Bramwell, *Helicopter Dynamics*. New York: John Wiley & Sons, 1976.
- [9] W. O. Miller and D. B. Bliss, “Direct periodic solutions of rotor free wake calculations,” *Journal of the American Helicopter Society*, vol. 38, pp. 53–60, April 1993.
- [10] S. Chu and S. E. Widnall, “Lifting-surface theory for a semi-infinite wing in oblique gust,” *AIAA Journal*, vol. 12, pp. 1672–1678, December 1974.
- [11] R. Martinez and S. E. Widnall, “Aerodynamic theory for wing with side edge passing subsonically through a gust,” *AIAA Journal*, vol. 21, pp. 808–815, June 1983.
- [12] J. S. Marshall, “Vortex cutting by a blade, part 1: General theory and a simple solution,” *AIAA Journal*, vol. 32, pp. 1145–1150, June 1994.
- [13] S. Lee and D. Bershader, “Head-on parallel blade-vortex interaction,” *AIAA Journal*, vol. 32, pp. 16–22, January 1994.
- [14] F. H. Schmitz and J. R. Grant, “Penetration of a blade into a vortex core: vorticity response and unsteady blade forces,” *Journal of Fluid Mechanics*, vol. 306, pp. 83–109, January 1996.
- [15] F. Farassat, “Linear acoustic formulas for calculation of rotating blade noise,” *AIAA Journal*, vol. 19, pp. 1122–1130, September 1981.

- [16] F. H. Schmitz and B. W.-C. Sim, “Acoustic phasing, directionality and amplification effects of helicopter blade-vortex interactions,” *Journal of the American Helicopter Society*, vol. 46, pp. 273–282, October 2001.
- [17] S. Glegg, W. J. Davenport, K. S. Wittmer, and D. S. Pope, “Broadband helicopter noise generated by blade wake interactions,” *Journal of the American Helicopter Society*, vol. 44, pp. 293–301, October 1999.
- [18] R. L. Bielawa, *Rotary wing Structural Dynamics and Aeroelasticity*. Washington: AIAA, 1992.
- [19] A. T. Conlisk, “Modern helicopter rotor aerodynamics,” *Progress in Aerospace Sciences*, vol. 37, pp. 419–476, 2001.
- [20] A. T. Conlisk, “Modern helicopter aerodynamics,” *Annu. Rev. Fluid. Mech.*, vol. 29, pp. 515–567, 1997.
- [21] F. H. Schmitz and Y. H. Yu, “Helicopter impulsive noise: Theoretical and experimental status,” *Journal of Sound and Vibration*, vol. 109, no. 3, pp. 361–442, 1986.

6 Figures

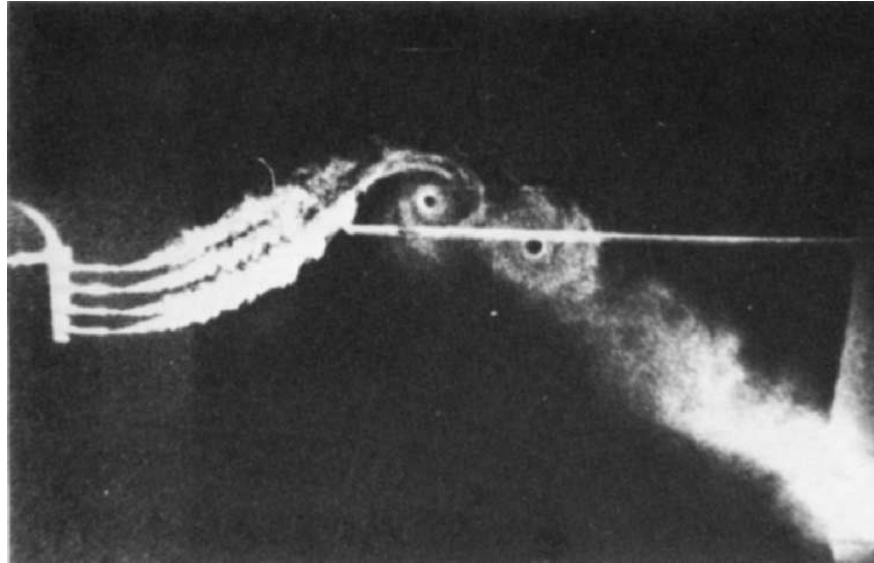


Figure 1: Flow through a Rotor (from Bramwell[8])



Figure 2: Flow through a Helicopter Rotor (from Bramwell[8])

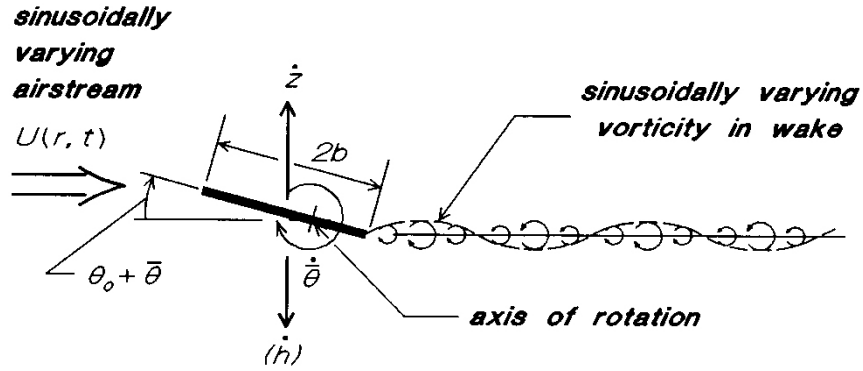
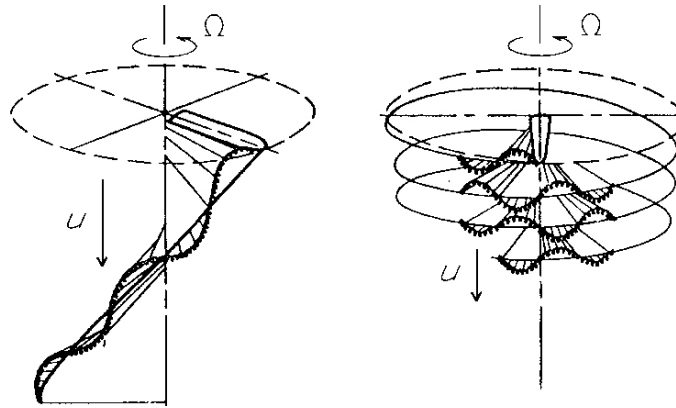
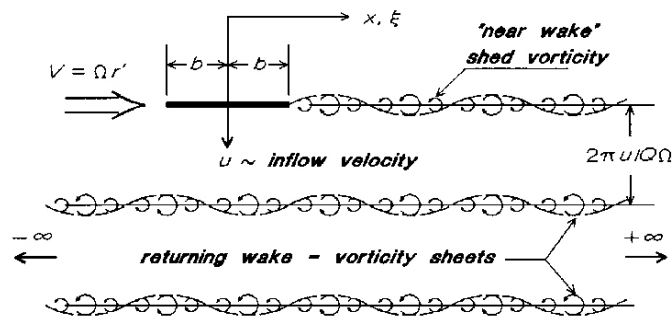


Figure 3: Isaacs Physics (from Bielawa[18])



(a) Rotor Flow Field (from Bielawa[18])



(b) 2D Loewy Wake Model(from Bielawa[18])

Figure 4: Loewy Function Physics

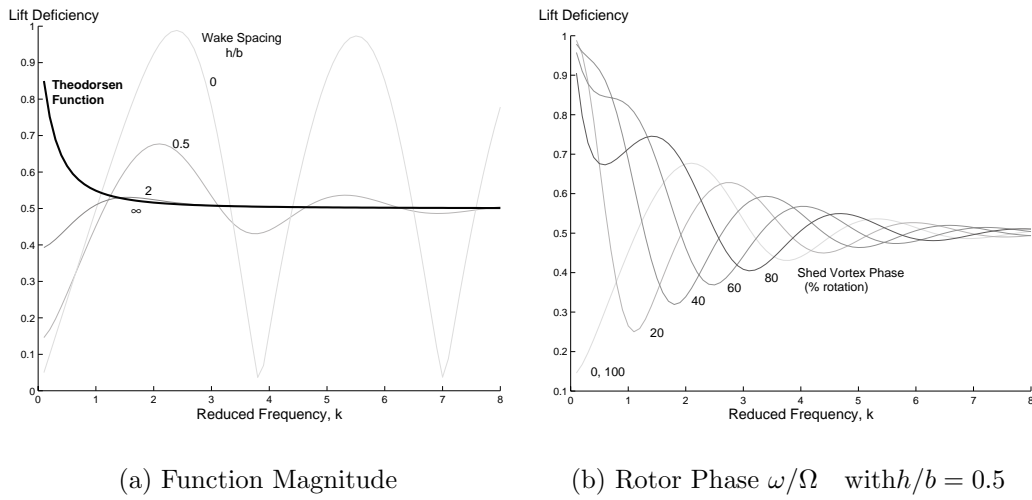


Figure 5: Loewy Function

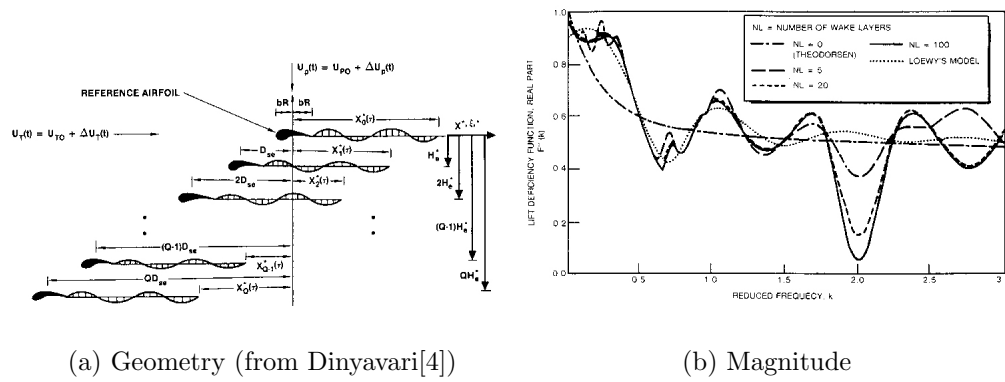


Figure 6: Rotor Cascade

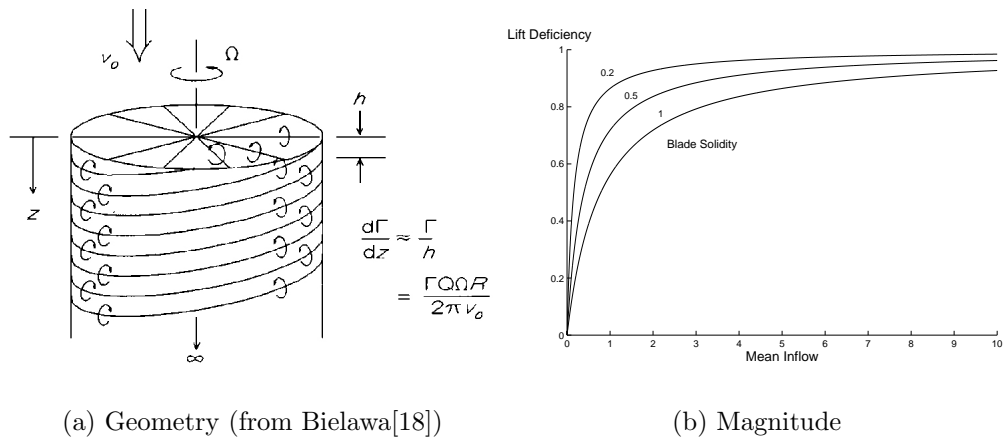


Figure 7: Miller Rotor Function

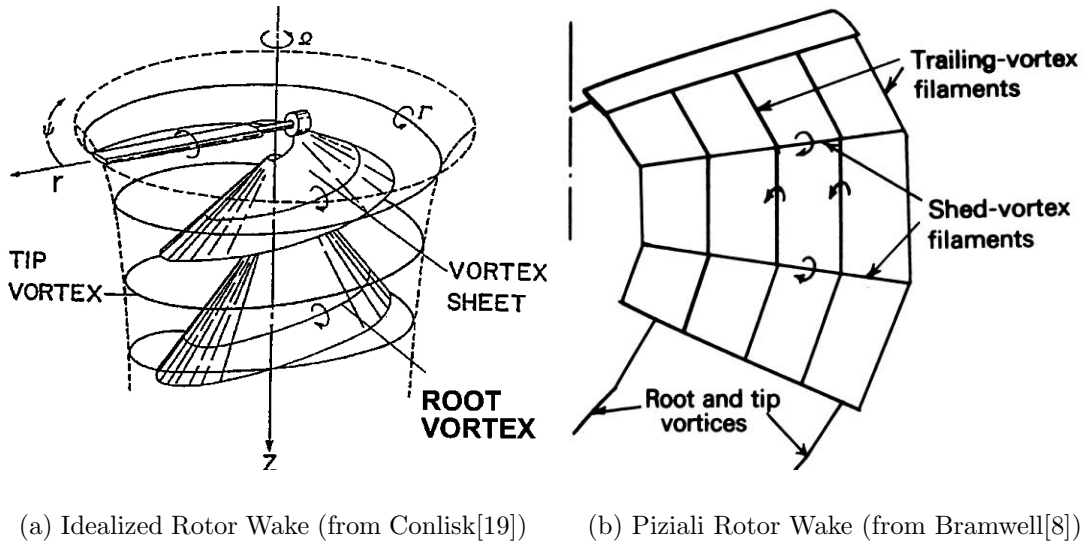


Figure 8: Rigid Discrete Vortex Methods

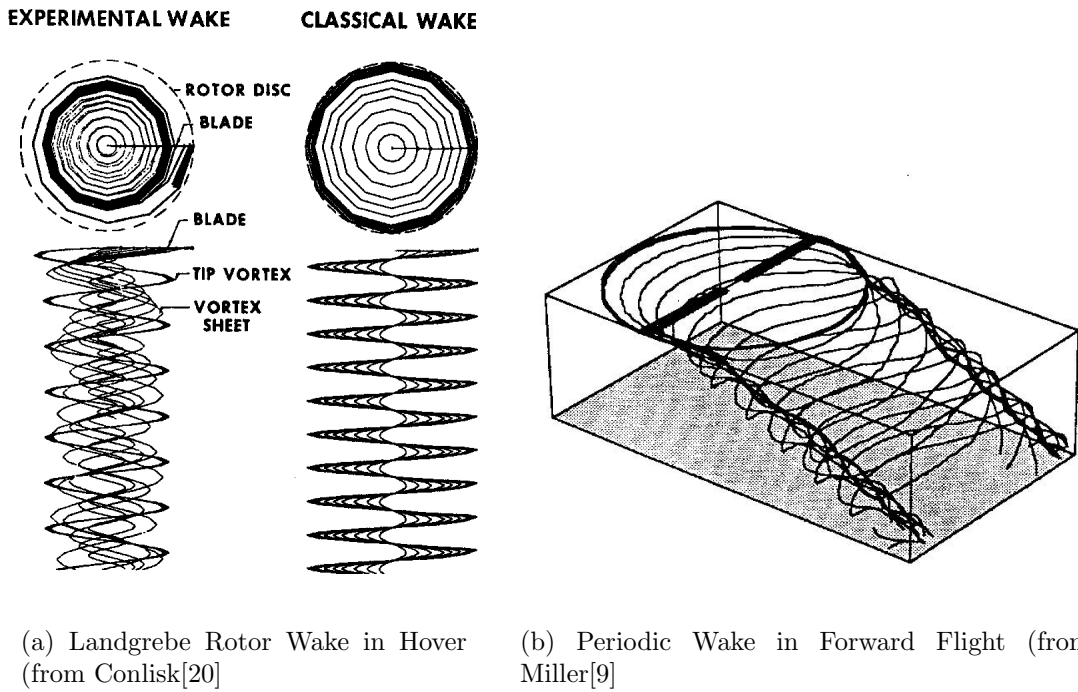


Figure 9: Free Discrete Vortex Methods

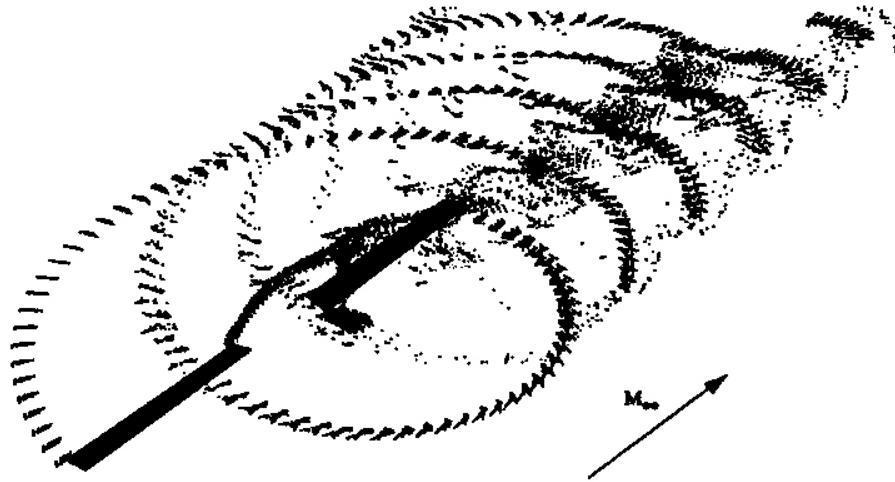
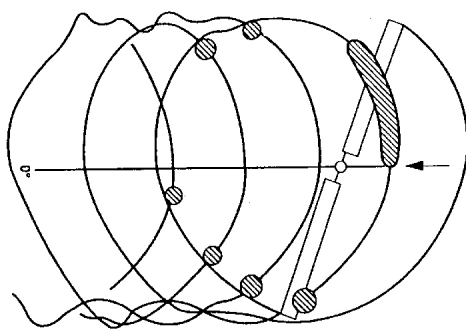
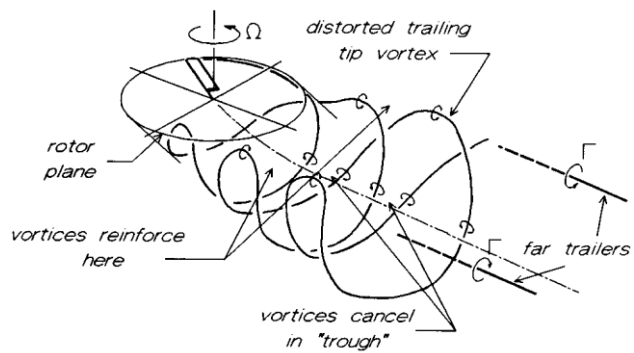


Figure 10: Rotor Wake Streaklines (from Conlisk[20])



(a) Idealized BVI (from Lee[13])



(b) Idealized Wake in Forward Motion (from Bielawa[18])

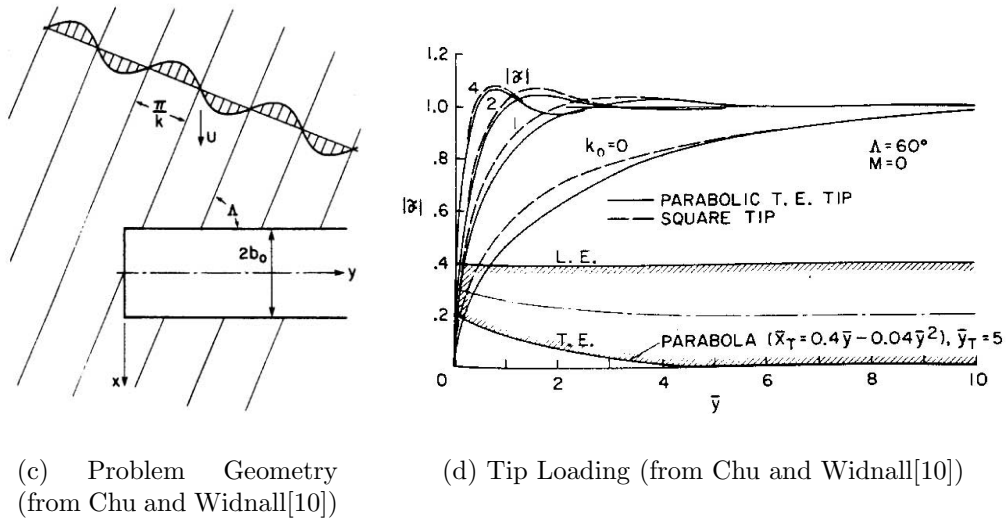


Figure 11: Oblique Gust

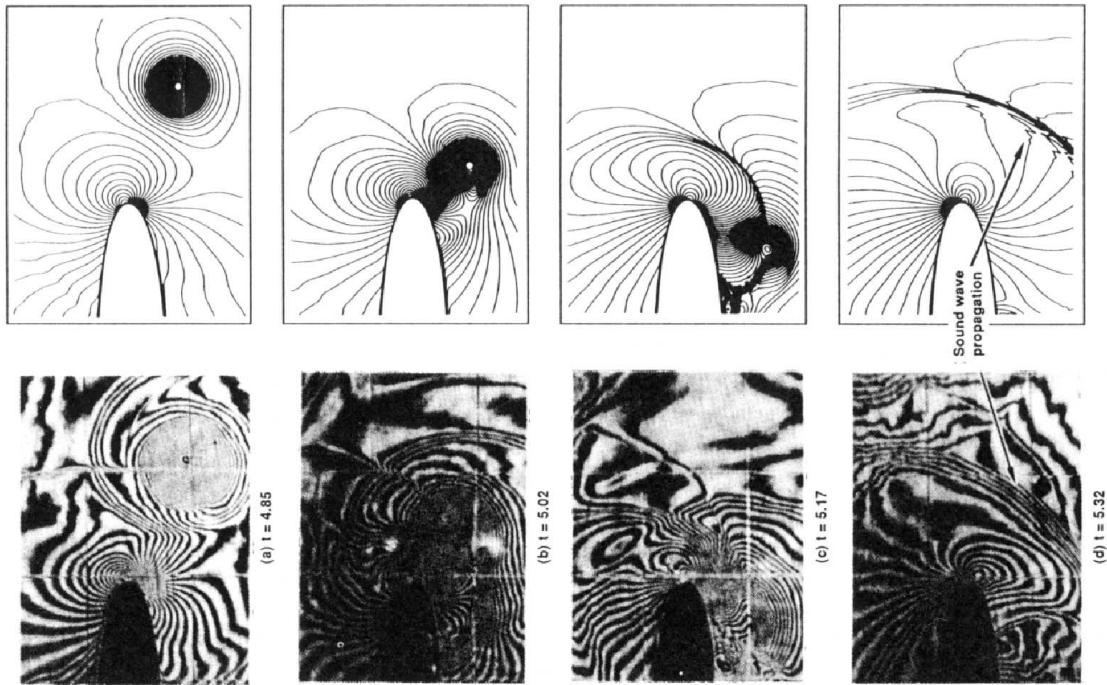


Figure 12: Experimental vs. Computational BVI $M=0.5$ (from Lee[13])

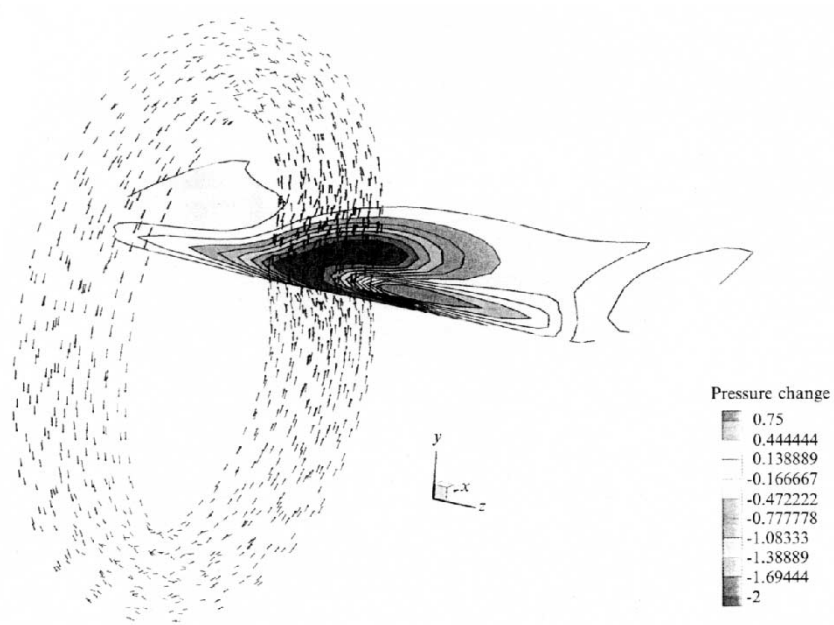


Figure 13: Computational BVI (from Marshall[14])

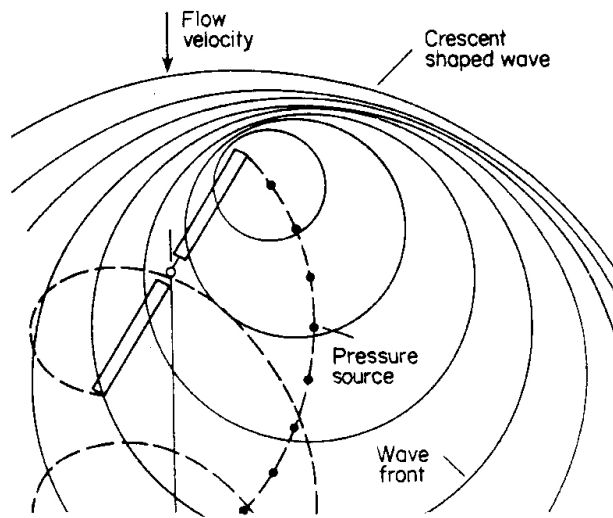
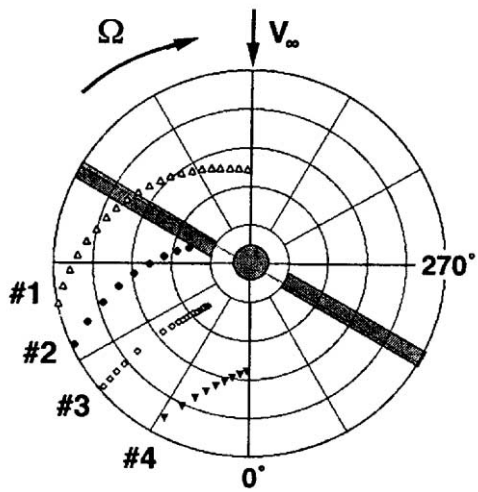
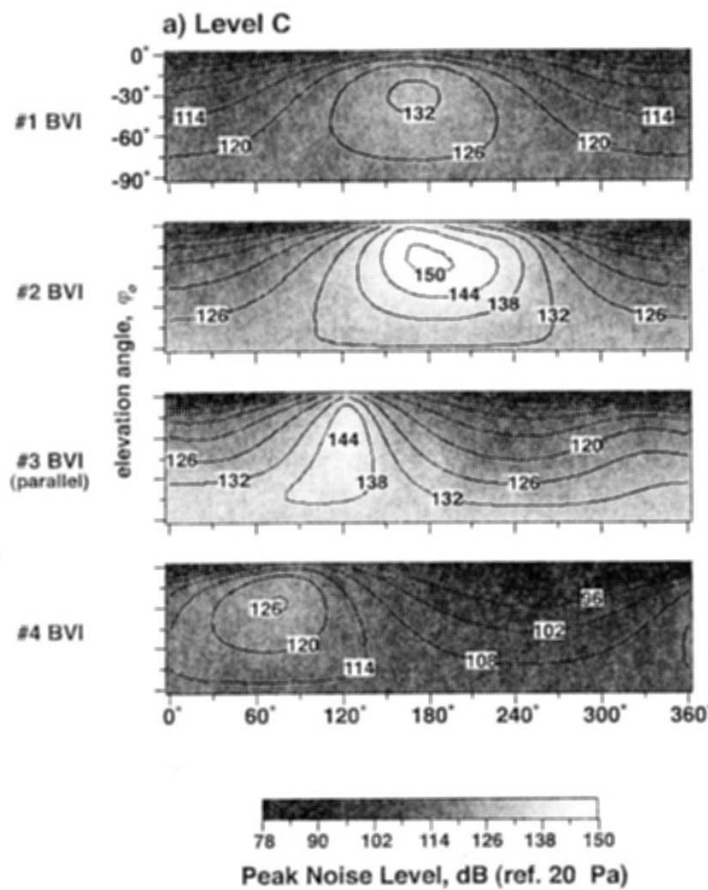


Figure 14: Advancing Blade Shock (from Schmitz and Yu[21])



(a) Problem Geometry (from Schmitz[16])



(b) Directivity Pattern (from Schmitz[16])

Figure 15: BVI Directivity